J Mater Sci (2008) 43:254–269
DOI 10.1007/s10853-007-2176-7

# Recent advances in shape memory polymers and composites: a review

**Debdatta Ratna · J. Karger-Kocsis**

Received: 27 April 2007 / Accepted: 18 September 2007 / Published online: 17 October 2007

**Abstract** Shape memory polymers (SMPs) belong to a class of smart polymers, which have drawn considerable research interest in last few years because of their applications in microelectromechanical systems, actuators, for self healing and health monitoring purposes, and in biomedical devices. Like in other fields of applications, SMP materials have been proved to be suitable substitutes to metallic ones because of their flexibility, biocompatibility and wide scope of modifications. The shape memory properties of SMPs polymers might surpass those of shape memory metallic alloys (SMAs). In addition to block copolymers, polymers blends and interpenetrating network structured SMP systems have been developed. The present review mainly highlights the recent progress in synthesis, characterization, evaluation, and proposed applications of SMPs and related composites.

## Abbreviations

| | |
|---|---|
| BD | Butanediol |
| BEBP | 4, 4′ Bis-(2-hydroxyethoxy) biphenyl |
| BHPP | 4, 4′ Bis-(2-hydroxyhexoxy) biphenyl |
| BIN | *N*,*N*-Bis-(2-hydroxy ethyl) isonicotinamide |
| CNT | Carbon nanotube |
| DMPA | Dimethylol propionic acid |
| $E_g$ | Glassy dynamic modulus |
| $E_r$ | Rubbery plateau modulus |
| HDI | Hexamethylene diisocyanate |
| HS | Hard segment |
| IPN | Interpenetrating polymer network |
| LC | Liquid crystalline |
| LRT | Lowest recovery temperature |
| MDI | 4,4′-Diphenylmethanediisocyanate |
| NMDA | *N*-Methyldiethamine |
| ODO | 1-Octadecanol |
| PCL | Polycaprolactone |
| PCLU | PCL-Based polyurethane |
| PDI | 1,6-Diphenyl diisocyanate |
| PE | Polyethylene |
| PEO | Polyethylene oxide |
| PET | Poly(ethylene terepthalate) |
| PGA | Polyglycolide |
| PGC | Poly(glycolide-co-caprolactone) |
| PLLA | Poly(L-lactide) |
| PMMA | Poly(methyl methacrylate) |
| PTMG | Poly(tetramethylene glycol) |
| PU | Polyurethane |
| $R_f$ | Shape fixity |
| $R_r$ | Shape recovery |
| SS | Switching segment |
| SMA | Shape memory alloy |
| SMP | Shape memory polymer |
| $T_g$ | Glass transition temperature |
| $T_m$ | Melting point |
| $T_r$ | Recovery temperature |
| $T_s$ | Switching temperature |

---

D. Ratna (✉) · J. Karger-Kocsis
Institute for Composite Materials, Technical University
of Kaiserslautern, Erwin-Schrödinger-Str. 58,
67663 Kaiserslautern, Germany
e-mail: ratnad29@hotmail.com

*Present Address:*
D. Ratna
Naval Materials Research Laboratory, Addl. Ambernath,
Thane 421506, India

## Introduction

The discovery of shape memory effect by Chang and Read in 1932 [1] is one of the revolutionary steps in the field of active materials research. Materials are said to show shape memory effect if they can be deformed and fixed into a temporary shape and recover their original permanent shape only on exposure of external stimuli like heat, light, etc. Thermally induced shape memory effect is more common where the recovery takes place with respect to a certain critical temperature. The most widely used shape memory material is Ni–Ti alloy (Nitinol) [2]. Shape memory alloys (SMA) exhibit outstanding properties such as small size, high strength and have found wide technical applications [3–8]. However, they have obvious disadvantages, such as high manufacturing cost, limited recoverable deformation and appreciable toxicity [9, 10]. Therefore, ceramic-based [11–13] and polymer-based [14–18] shape memory materials have been explored.

The shape memory polymers (SMPs) have drawn increasing attention because of their scientific and technological significance [16–18]. They offer deformation to a much higher degree and a wider scope of varying mechanical properties compared to SMAs or ceramics, in addition to their inherent advantages of being cheap, light weight, and easy processability. Polymers offer extra advantages due to the fact that they may be biocompatible, nontoxic, and can be made biodegradable.

Shape memory polymer was first developed by CDF Chimie Company (France) in 1984 under the trade name of Polynorbornene [19]. After that lot of works have been done and various kinds of SMPs have been reported and developed which will be reviewed shortly. SMP can be designed by taking a polymer material, in which the polymer chains are able to fix a given deformation by cooling below a certain transition temperature ($T_s$). The transition temperature ($T_s$) can be the glass transition or the melting point of the polymer. Melting point is preferred over the glass transition as melting is comparatively a sharper transition. Upon reheating to above $T_s$, the oriented, or crystalline chains in the network, restore the random coil conformation resulting in a macroscopic recovery of the original shape. The process is shown schematically in Fig. 1. Such polymer systems consist of two segments/phases; one of them is a fixed phase and the another is a reversible or switching one. The permanent shape is given either by physical or chemical crosslinks. A schematic representation of the micromechanisms describing shape memory action is shown in Fig. 2. On the basis of the nature of crosslinks, SMPs are subdivided into two categories: physically crosslinked SMP and chemically crosslinked SMP. On the basis of nature of switching segments, SMPs are subdivided into two categories: SMP with amorphous switching segment ($T_s = T_g$ ) and SMP with crystalline switching segment ($T_s = T_m$).

Shape memory is usually a thermally induced process, though it can be triggered electrically [20], magnetically [21] or electromagnetically [22] provided that the corresponding polymer contains a suitable active filler. For the filled composites, the fillers are activated by electric, magnetic or electromagnetic stimuli and thereby thermal effect is generated, which induces the recovery process. Finkelmann and coworker [23, 24] reported shape memory liquid crystalline (LC) elastomer, which can be stimulated by photo-illumination by incorporating azo groups into the LC mesogens. Upon UV-radiation, the azo groups isomerized from the trans to the cis configuration and sharply bent the mesogens, hampering the nematic ordering. Correspondingly, the material underwent a photo-induced nematic-isotropic transition, accompanied with a large shape change. Recently, Lendlein et al. [25] reported a novel light-induced SMP by introducing molecular switches such as cinnamic acid [26] and cinnamylidene acetic acid [27]. The latter compounds are able to undergo efficient photoreversible [2 + 2] cycloaddition reactions when exposed to alternating wavelengths ($\lambda > 260$ nm or $\lambda < 260$ nm)]. The temporary shape is fixed owing to the formation of new photo-responsive crosslinks and the photo responsive crosslinks can be reversibly cleaved by irradiation with UV light of $\lambda < 260$ nm, leading to recovery of the original shape. The unique characteristics of the above mentioned SMP systems, enable the manipulation of the shape recovery at ambient temperatures by remote activation and elimination of temperature constraints for medical and other applications arising from external heating.

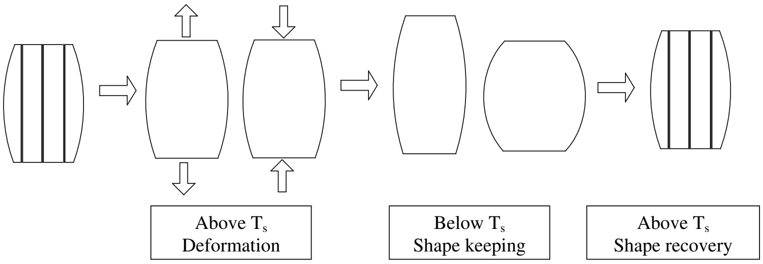

**Fig. 1** Schematic representation of a macroscopic shape memory effect

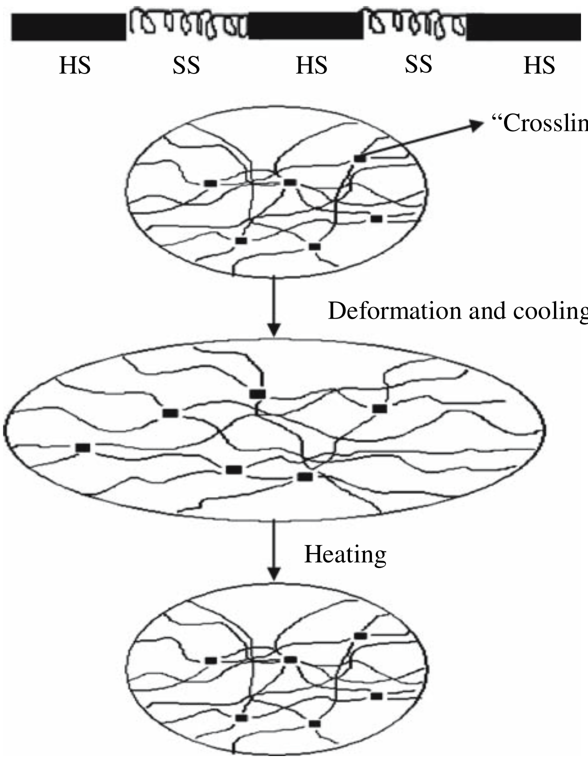

**Fig. 2** Micromechanism of shape memory effect of polymers

## Properties of SMPs

The important quantities to be determined for describing shape memory properties of a material are the strain recovery rate ($R_r$) and strain fixity rate ($R_f$). The strain recovery rate qualifies the ability of the material to memorize its permanent shape, whereas strain fixity rate describes the ability of the switching segment to fix the mechanical deformation. A description of a thermomechanical test with loading at high temperature is shown in Fig. 3. A sample is deformed to a constant strain $\varepsilon_m$ at a constant strain rate. While maintaining the strain at $\varepsilon_m$, the samples were cooled to a low temperature and unloaded. Upon removing the constraint under cooled condition, a substantial recovery of strain $\varepsilon_u$ occurs. The sample was subsequently heated above $T_s$ and kept at that temperature allowing the recovery to take place. This completes a thermomechanical cycle leaving a residual strain $\varepsilon_p$. The $R_r$ and $R_f$ for $N$th cycle can be determined from the following formula:

$$R_r(N) = \frac{\varepsilon_m - \varepsilon_p(N)}{\varepsilon_m - \varepsilon_p(N-1)}$$

$$R_f(N) = \frac{\varepsilon_u(N)}{\varepsilon_m}$$

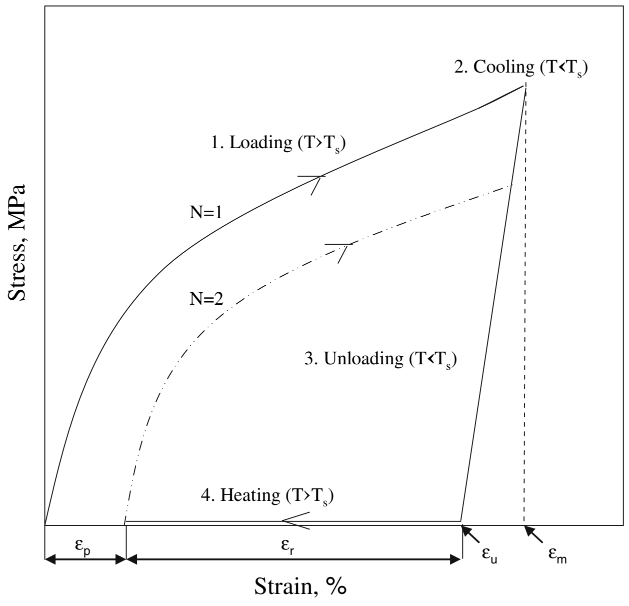

**Fig. 3** Graphical description of a thermomechanical test

The shape memory effect in metals and ceramics originates from a phase transformation phenomenon, which is associated with a change in volume [9, 10]. Deformations of the low temperature phase, occurring above a critical stress, are recovered completely during the solid–solid transformation to the high temperature phase. Whereas, the driving force for shape recovery in a polymer, is the elastic strain generated during the deformation [28]. Deformation at high temperature is much easier due to the lower rubbery modulus of the polymer that makes the orientation of polymer more feasible. However, the orientation will be partly relaxed before the structure is frozen in during the subsequent cooling cycle. On the other hand, deformation at low temperature is more difficult due to the higher glassy state modulus of the polymer but chain orientation will remain at a higher degree as the relaxation process is slowed down. A high glassy state modulus ($E_g$) will provide the material with a high shape fixity during simultaneous cooling and unloading, whereas a high rubbery modulus ($E_r$) will provide high elastic recovery at high temperature. Various viscoelastic and thermomechanical models have been studied to correlate the viscoelastic/thermal properties with the shape memory behavior [29–34].

Shape memory effect can be described briefly as the following mathematical model [35]:

$$\text{Shape fixity ratio } R_f = 1 - E_r/E_g$$

$$\text{Shape recovery ratio } R_r = 1 - f_{IR}/[(1 - E_r/E_g)f_\alpha]$$

where $E_g$ is the glassy modulus, $E_r$ is the rubbery modulus, $f_{IR}$ is the viscous flow strain and $f_\alpha$ is the strain when $t >> t_r$. A high elasticity ratio ($E_g/E_r$) allows for an easy shaping at $T > T_s$ (shape memory temperature) and a great resistance to the deformation at $T < T_s$. The polymer material has to be designed to meet the above criteria for shape memory applications. Typical dynamic modulus versus temperature plots of a thermosetting type ordinary polymer and a crosslinked shape memory polymer, are shown in Fig. 4.

## Physically crosslinked SMPs

### SMP with amorphous switching segment

Shape memory effect has been reported for various polymers like poly(methyl methacrylate) [36], polynorbornene [37–39], poly(methylene-1,3 cyclopentane) [40]. Since their discovery by Mitsubishi Heavy Industries Ltd., in 1988, extensive research on segmented polyurethane (PU) has been carried out [41–46]. Recently, Baer et al. [47] studied the effect of processing parameters on the thermomechanical properties of commercially (Mitsubishi) available PU-based materials. There was a significant variation in rubbery modulus for the sample cooled at different rates during the processing. Thus thermomechanical properties of these materials can be adjusted for various medical applications. The thermal and dynamic mechanical properties of Mitsubishi PU materials are given in Table 1. The exact compositions of these SMPs have not been published, but they seem to consist of a complex combination of short amorphous polyester and polyether soft segments, short diol extender and aromatic urethane hard segments. The materials were synthesized by polymerizing alternatively hard segment (diphenylmethane diisocyanate) and soft segment (polyol) and various interactions among the segments leaded to the domain formation; hard segment worked as pivoting point for shape recovery and soft segment could mainly absorb external stress applied to the polymer. Hu et al. [48] investigated the effect of thermomechanical cyclic conditions on shape memory properties of a PU-based SMP (Mitsubishi-MS 4510). The recovery ratios increased with increasing deformation speed and with decreasing maximum strain. Hence, in order to achieve good-shape memory properties, deformation of the samples should be fast. In addition, it should be noted that too high a deformation amplitude would render the shape memory effect unsatisfied.

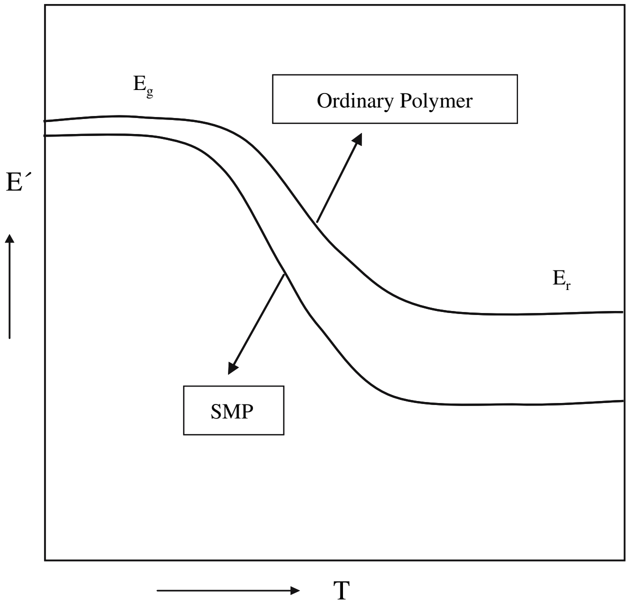

**Fig. 4** Typical dynamic modulus versus temperature plots of an ordinary crosslinked polymer and SMP

The $T_g$ of thermoplastic PU materials could be controlled in a wide range from –30 to 100° C by using different kinds of urethane ingredients (diisocyanate, polyol, and chain extenders) and by adjusting their molar ratios [49–62]. In order to have effective shape memory property, the glassy hard segments should maintain the shape through inter- or intra-polymeric chain attractions, such as hydrogen bonding or dipole–dipole interaction, together with the physical crosslinking, but soft segments could freely absorb external stress by unfolding and extending their molecular chains. If the stress exceeds and breaks the interactions among hard segments, shape memory will be lost and original shape cannot be restored. Therefore, precise control of composition and structure of hard and soft segments is very important to satisfy the conditions required for various applications. In the segmented PUs the hard segment (HS) acts as the physical crosslink and hard segment concentration should be sufficiently high (>20 wt%) in order to generate a shape-memory effect [53]. Optimum shape memory properties were achieved at 35–40 wt% of HS concentration (Fig. 5). For a fixed molar composition, the HS content increases with decreasing molecular weight of polyol [55] as shown in Fig. 6, for a poly(tetramethylene glycol) (PTMG)/4,4′-diphenylmethane diisocyanate (MDI)/1,4-butane diol (1,4-BD) system.

The compositions and properties of different types of PUs reported in recent literature are summarized in Table 2. Wang and Yuen [58] synthesized a series of thermoplastic PUs using aromatic chain extenders such as 4,4-bis(4-hydroxyhexoxy)-isopropylene or naphthoxy diethanol, in addition to 1,4-BD and reported an improvement in shape memory properties as a result of introduction aromatic structure into the main chain. Yang et al. [59] compared the mechanical, dynamic mechanical and shape memory properties of PU block copolymers with

**Table 1** Thermal and viscoelastic properties of DiAPLEX® (Mitsubishi) SMPs [47]

| Trade | Type | $T_s$ °C | $T_g^a$ °C | Tan $\delta^b$ peak temperature °C | $E_g^b$ Pa | $E_r^b$ Pa |
|---|---|---|---|---|---|---|
| MM5510 | Thermoplastic | 55 | 51 | 54.9 | 8.1E8 | 1.6E6 |
| MM4520 | Thermoplastic | 45 | 36 | 45.9 | 6.6E8 | 1.3E6 |
| MM5520 | Thermoplastic | 55 | 46 | 57.3 | 7.7E8 | 1.4E6 |
| MM6520 | Thermoplastic | 65 | 65 | 66.6 | 8.9E8 | 2.1E6 |
| MM7520 | Thermoplastic | 75 | 74 | 74.6 | 7.7E8 | 1.8E6 |
| MP3510 | Thermoset | 35 | 31 | 46.1 | 5.2E8 | 1.6E6 |
| MP4510 | Thermoset | 45 | 42 | 54.1 | 7.0E8 | 1.7E6 |
| MP5510 | Thermoset | 55 | 52 | 65.2 | 8.1E8 | 1.9E6 |

[a] Determined by differential-scanning calorimetry

[b] Determined by dynamic-mechanical analysis

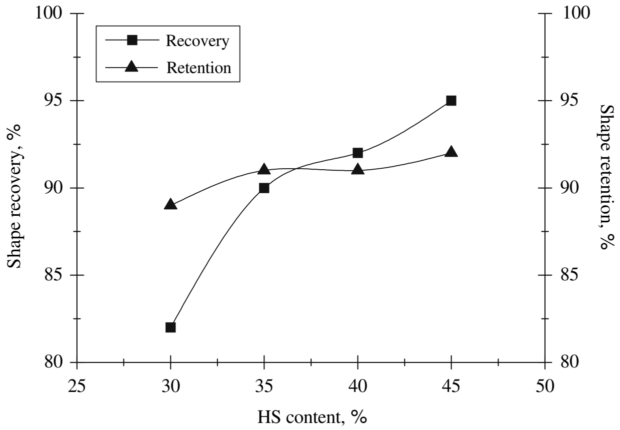

**Fig. 5** Shape recovery and shape retention data [53] of PU-based SMPs plotted against HS concentration

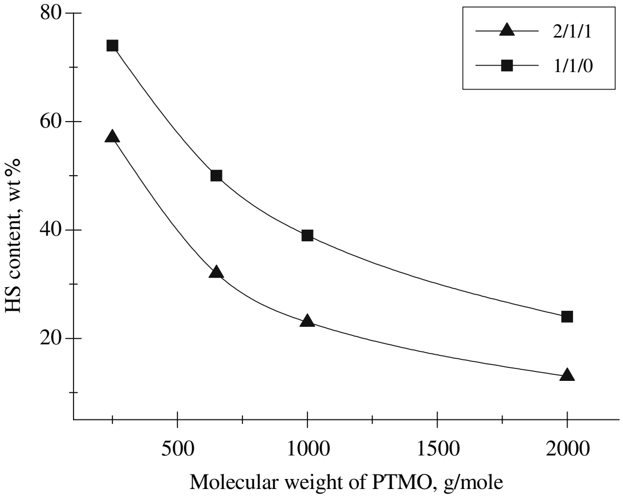

**Fig. 6** HS content data [55] plotted against molecular weight of polyol at different polyol/MDI/1,4-BD ratios

planar shape HS (1,6-diphenyl diisocyanate-PDI) and bent shape HS (MDI). The PDI-based PU shows superior property compared to MDI-based PU (Table 2) as a result of better interaction among hard segments due to the planar shape of PDI.

Water vapor permeability and mechanical properties of PU-based SMP coatings were investigated [60] and the studies show that water vapor permeability was mainly influenced by the concentration of coating solution and the mechanical property was influenced by the PU hard segment content. Yang et al. [61] carried out a systematic study on the effects of moisture on the glass transition temperature and thermomechanical properties of a polyether-based PU. The results reveal that the hydrogen bonding between N–H and C = O groups is weakened by the absorbed water which resulted in considerable deterioration of shape memory properties. Attempts have been made to convert the PU-based-SMPs into conventional melt spun [63] and electrospun [64] shape-memory fibers. The drawn fiber shows better shape memory properties compared to spun fibers due to the formation of oriented hard segment regions, which are strongly bonded with H-bonds [63]. The electrospun fiber of PU-based SMP with 50 wt% hard segment [53] shows more than 80% shape recovery [64].

Blending of PU with other polymers like poly(vinyl chloride) (PVC) [65], phenoxy [66], as a means to meet the demands of improved mechanical properties and adjustment of $T_s$, has been investigated. The can be adjusted by changing the blend compositions. However, open literatures about shape memory effect of polymer blends are limited [65–67]. The probable reason for lack of interest is the versatile PU chemistry. This offers a wide scope for tailor-making the properties of such materials, as discussed in previous sections thus there is no need for alternating strategies, such as blending.

## SMPs with crystalline switching segment

Shape memory polymers with amorphous soft phase (especially segmented polyurethanes—discussed in

**Table 2** Compositions and properties of physically crosslinked segmented PUs (amorphous soft phase)

| Polyol Mw, g/mole | Isocyanate | Extender | HS wt% | $T_g$ °C | $R_r(1)$ % | $R_f(1)$ % | References |
|---|---|---|---|---|---|---|---|
| PTMG 650 | MDI | 1,4-BD | 31–86 | –13 to 38 | 95 | – | [54] |
| PTMG 2000 | MDI | 1,4-BD | 12–50 | – | 90% | – | [55] |
| PTMG | MDI | 1,4-BD | 20–50 | –15 to 2 | 95 | 91 | [53] |
| PTMG | MDI | 1,4-BD | 30–35 | 0 to –15 | 85 | – | [59] |
| PTMG | PDI | 1,4-BD | 20–25 | –1 to –17 | 96 | – | [59] |
| PTMG 1000,2000 | MDI | 1,4 BD + BES + BPE/ND | 52–73 | 83–107 | >90 | – | [58] |
| BHBP | TDI + HDI | 1,3-BD | 21–41 | 10–35 | | | [56] |
| PTMG 1800 | MDI | 1,4-BD | 30 | –10 | >80 | 90 | [60] |
| PTMG 1000,2000 | MDI | 1,4-BD | 35 | –10 to 30 | >80 | >80 | [57] |

*Note*: $R_f(1)$ and $R_r(1)$ indicate optimum values of shape fixity and shape recovery respectively after first recovery

previous sections) have the advantages that they are able to store in principle more elastic energy. However, the adjustment $T_g$ to a certain temperature for a specific application, is not straight-forward and usually requires a judicious selection of a combination of soft segments [49–62]. Another alternative is to use a soft segment that crystallizes below $T_s$. Such SMPs show a narrow transition zone, unlike the SMPs, with amorphous reversible segments, which often show broad-transition temperature range.

Various SMP compositions, with crystalline reversible segments, and their shape memory properties are presented in Table 3. The shape memory properties evaluated under different conditions are difficult to compare, hence, the optimum values have been reported. Polycaprolactone (PCL) has been extensively used for synthesis of PU with crystalline soft phase. PCL is first converted to PCL diol (reaction scheme shown in Fig. 7) and the diol is used to synthesize the PU-based SMPs [68, 69]. The PCL segment undergoes microphase separation and forms the soft-switching segment. The recovery temperature, $T_r$ (the temperature at which fast recovery takes place) can vary from 40 to 60° C depending on the soft phase/hard phase composition and molecular weight of PCL. The relation between the shape memory effect and molecular structure has been investigated and it was concluded that high crystallinity of the soft-segment-region at room temperature was a necessary prerequisite for segmented PUs to demonstrate shape-memory behavior [70, 71]. However, the crystallization of PCL segments is hindered by incorporating them into the multiblock copolymers. No crystallization was observed when PCL-diol has a number average molecular weight less than 2000 g/mole and the optimum molecular weight in terms shape memory properties was found to be 5000–6000 g/mole [35, 71] (Fig. 8).

In cyclic thermomechanical measurements, it was found that the initial slope increases with increase in number of cycle (during initial few cycles) unlike that observed in PU with amorphous switching phase. The behavior can be attributed to the relaxation of the material in the stretched state which results in an increasing orientation and crystallization of the chains. The studies on water vapor

**Table 3** Structure and properties of physically crosslinked SMPs with crystalline soft phase

| Hard segment | SS | % SS | $T_r$ °C | $R_f(1)/R_f(4)$ % | $R_r(1)/R_r(4)$ % | References |
|---|---|---|---|---|---|---|
| MDI/1,4-BD | PCL | 70 | 44–55 | 82/95 | 82/73 | [70] |
| MDI/1,4-BD | PCL/PVC blend (6/4) | 38–62 | 18–48 | 92 | 60 | [71] |
| HDI/4,4′-dihydroxybiphenyl | PCL | 30–80 | 38–58 | 90 | 85 | [74] |
| MDI/BEBP or BHBP | PCL | 57–70 | 41–50 | 80/85 | 80/75 | [75] |
| MDI/DMPA | PCL | 70 | 45 | 95/95 | 66/45 | [76, 77] |
| MDI/NMDA or BIN | PCL | 75 | 10–20 | 98 | 90 | [79] |
| Aramid | PCL | 78–91 | 14–54 | 78 | 99 | [80] |
| MDI/1,4-BD + ODO | PBAG | 75 | 40–45 | ~100 | ~100 | [78] |
| TDI/1,4-BD | Trans-polyisoprene | 70 | 65 | 99 | 85 | [83, 84] |
| PET | PEO | 72 | 58 | >90 | – | [85–87] |

*Note*: $R_f(1)$ and $R_r(1)$ indicate optimum values of shape fixity and shape recovery, respectively, after first cycle

$R_f(4)$ and $R_r(4)$ indicate optimum values of shape fixity and shape recovery, respectively, after fourth cycle

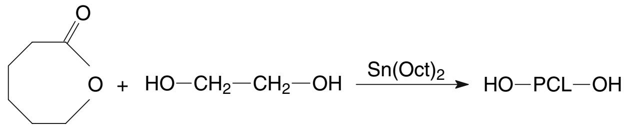

**Fig. 7** Reaction scheme for synthesis of PCL-diol

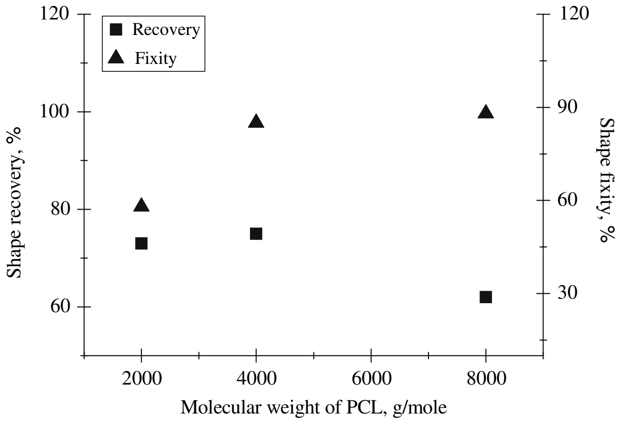

**Fig. 8** Shape-recovery and shape-retention data [35] of PU-based SMPs ploted against molecular weight wt of PCL

permeability of crystalline SMPs [72, 73] indicate different behavior compared to amorphous soft phase containing PUs (discussed in earlier sections). A phenomenon of temperature sensitive water vapor permeability at soft segment crystalline melting point was observed. When the experimental temperature reached the soft segment crystalline melting temperature, an abrupt change in water vapor permeability of PU coated fabrics was observed. The significant change of water vapor permeability of PU coated fabrics, is due to the phase change of PU, which causes density changes inside the membranes due to micro-Brownian motion of soft segment, therefore, enhanced the water vapor permeability through the coated fabrics. The water vapor permeability of the coated fabrics, was also dependent on the primary structure of PU and increase with the introduction of hydrophilic groups.

The major issues related to the developments of such PU-based SMPs are to achieve maximum crystallization and stable-hard segment domains. Various strategies like incorporation of mesogenic segment [74, 75], ionic groups [76, 77], and long alkyl chain [78] have been adopted to enforce microphase separation (Table 3). Mesogenic segments were incorporated in the PU by partially replacing 1,4-BD in PU formulation by 4,4′-bis(2-hydroxyethoxy)biphenyl (BEBP) or 4,4′-bis(2-hydroxyhexoxy)biphenyl (BHPP). The improvement in solubility and shape fixity (Table 3) were observed as a result of incorporation of mesogenic groups. Influence of ionic groups on the crystallization behavior of segmented PU using PCL-diol of various molecular weights (4,000, 20,200, 58,500, and 71,600 g/mole) was also investigated [77]. Ionomers were synthesized by using dimethylol propionic acid (DMPA) in addition to 1,4 BD. Crystallization studies indicate that crystallization rate increases as a result of incorporation of ionic groups in case of PU made from PCL-4000, whereas in case of samples having higher molecular weight of PCL the crystallization rate increases. The inomers show higher tensile strength, modulus and fatigue resistance compared to the corresponding non ionomers due to the columbic forces among the ionic centers within the polymer backbone.

Zhu et al. [79] synthesized PCL-based PU cationomer by partially replacing 1, 4 BD by an extender with ammonium ions in the backbone or as pendent group. They used *N*-methyldiethamine (NMDA) or *N*,*N*-bis(2-hydroxyethyl)isonicotinamide (BIN) as an extender and the corresponding cationomers were synthesized by neutralization of NMDA or BIN with stoichimetric amount of acetic acid. Introduction of cationic groups (6–8 wt%) resulted in improved crystalisability in both the cases, however, significant improvement in shape memory properties was observed in case NMDA-based PU. This indicates that the content and category of cationic groups have deep influences on the shape memory properties of PU.

The effect of incorporation of low-molecular weight lubricants, such as 1-octadecanol (ODO) and liquid paraffin on the microphase separation and antiplasticiza tion of PU, were investigated [77, 80, 81]. ODO molecules are capped at the end of poly(1,4 butylene adipate) glycol (PBAG)-based PU, via a urethane reaction between isocyanate capped PU prepolymers and hydroxyl groups of ODO. The long alkyl chains of ODO are dispersed at the interface of two phases in a PU system because of immiscibility. This facilitates the microphase separation and resulted in an improvement of shape memory properties [77]. Shape fixity and shape recovery close to 100%, were achieved by incorporating only 0.6 wt% ODO into the PU structure. Similar effect was achieved by using liquid paraffin, however, the effect was found to be less prominent in case physical blending with liquid paraffin.

Rabani et al. [82] synthesized PU (SMP) with aramid hard segment by reacting a diamine (instead of isocyanate) with PCL-diol. The unique feature of this class of PU is that they provided effective physical crosslinks even at a low-hard segment content (less than 15 wt%). Shape memory effects have also been reported for SMPs with other crystalline phases. Typical examples are trans-poly-isoprene-based PU [83,84] and polyethylene oxide (PEO)/poly(ethylene terepthalate) (PET) [85–87] as presented in Table 3. The melting point of PEO varies from 45 to 65° C, depending on the molecular weight. However, the melting point of PEO of same molecular weight (in the block copolymer) decreases with increasing PET content due to the steric-hindrance for the crystallization process typically observed in block copolymers.

## Chemically crosslinked SMP

The limitation of physically crosslinked polymer in terms of the shape memory applications is that they are prone for creep and for some irreversible deformation during "memory programming." Polymer network-based SMP can be synthesized by either adding multifunctional crosslinker during the polymerization or by subsequent crosslinking of a linear or a branched polymer [88–91]. The polymer or blends namely polyethylene [88], polyethylene/poly(vinyl alcohol) and polyethylene/polyamide blends [89], and poly(vinyl chloride) [91], exhibit shape memory property, when they are suitably crosslinked. The shape memory effect has also been investigated for $\gamma$-radiation crosslinked PCL [92]. The crosslinked PCL has a higher tensile modulus and heat resistance and shows an elastic state. So it can be stretched and deformed at about 60 °C and after cooling to room temperature, the deformation can be maintained effectively. When heated again the strain can recover back to the original shape. In order to improve the radiation-crosslinking efficiency, the blends of PCL and polyfunctional acrylate monomers have also been investigated [93].

Recently, shape memory effects have been reported for copolymer of corn oil, styrene and divinylbenzene [94, 95], filler-modified epoxy [32] and epoxidized natural rubber crosslinked with 3-amino-1,2,4-triazole [96]. Rousseau and Mather [97] reported a smectic liquid crystalline (LC) elastomer based shape memory polymer. The structure of LC moieties used is shown in Fig. 9 Above the isotropization temperature, the relaxed state of elastomer (whose shape was acquired during crosslinking) can be easily deformed to tensile strain of about 300%. Subsequent fixing of this secondary shape is possible by cooling to the smectic LC phase. This LC elastomer features a sharp transition close to the body temperature, a low modulus comparable to muscle and optical clarity.

### Crosslinked polyurethanes

Crosslinked polyurethanes were made by using excess diisocyanate or by using a crosslinker like glycerin, trimethylol propane [98–100]. In case of PU with crystalline soft segments, the crosslinking (introduced in the structure), decreases the crystallization of the soft segment and upgrades the mechanical properties of the resulting crosslinked structure (Table 4). Buckley et al. [101] reported a novel thermosetting PU using 1,1,1-trimethylol propane as a crosslinker. Improvement in creep, increase in recovery temperature and recovery window, were observed due to introduction of the crosslinking. Xu et al. [102] synthesized hybrid PU, crosslinked with Si–O–Si linkages, formed through hydrolysis and condensation of ethoxy silane groups. The Si–O–Si linkages, not only act as the netpoints but also act as inorganic fillers for reinforcement. Thermosetting PU with both shape memory and hydrogel properties were also investigated [103, 104]. They can be made by making graft copolymers, of PU and other hydrophilic polymers, for example polyacrylamides, polyacrylates or by introducing hydrophilic groups into the crosslinked PU backbone [103, 104].

## PEO-based crosslinked SMP

The reports on PEO-based crosslinked SMPs are summarized in Table 5. Effect of crosslinking on the properties of PEO–PET block copolymers (discussed in earlier sections), have been investigated [105, 106] (Table 5). Maleic anhydride, glycerin or dimethyl 5-isopthalates, have been used as the crosslinkers. It was reported that addition of 1.5 wt% maleic anhydride, resulted in an increase in shape recovery from 35% to 65% and tensile strength from 3 to 9 MPa [105]. The crosslinked polymers have also been used to make high impact composites [107].

A successful development of SMP covers the followings: to set an optimum recovery rate, possibility to manipulate the recovery temperature upon the target applications (recovery temperature must lie below that of the system temperature) and ensure adequate thermomechanical properties. Most of the SMP reported, so far are

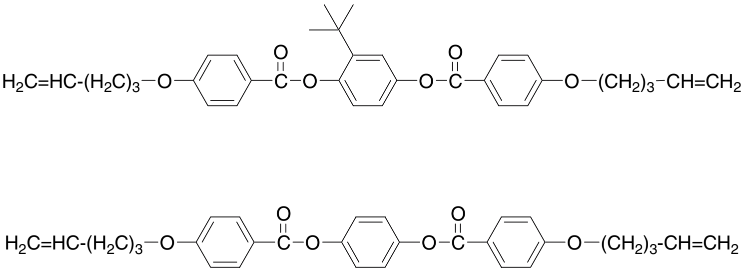

**Fig. 9** Chemical structure of LC moiety of an LC-based SMP

**Table 4** Effect of crosslinking on mechanical and shape memory properties of crosslinked PUs [98, 99]

| Hard phase | Soft phase | Crosslinker | E′ GPa | $\sigma$ MPa | $T_m$ °C Soft phase | $R_f$ (5) % | $R_r$ (5) % |
|---|---|---|---|---|---|---|---|
| MDI,1,4-BD, DMPA | PCL Mn ~ 4000 | Nil | 0.2 | 18 | 50.3 | 80 | 75 |
| MDI,1,4-BD, DMPA | PCL Mn ~ 4000 | Glycerin 6 wt% | 0.5 | 40 | 46.9 | 90 | 88 |

*Note*: $R_f(5)$ and $R_r(5)$ indicate optimum values of shape fixity and shape recovery, respectively, after fifth cycle

E′ and $\sigma$ are storage modulus and tensile strength respectively, at room temperature

**Table 5** PEO-based chemically crosslinked SMPs

| Hard phase | Crosslinker | $T_r$ °C | $R_f$ (5)% | $R_r$(5)% | References |
|---|---|---|---|---|---|
| PET | Glycerol/dimethyl 5-sulfoisopthalate | 11–30 | 90–95 | 60–70 | [105, 107] |
| PET | Maleic anhydride | 8–18 | 91–93 | 60 | [106] |
| AA/MMA copolymer | *N*,*N*′-methylene-bis-acrylamide | 90 | – | 99 | [108] |
| MMA/*N*-vinyl-2 Pyrrolidone | Ethyleneglycol Dimethacrylate | 90 | – | 99 | [109] |
| PMMA | Ethyleneglycol Dimethacrylate | 45,100 | – | 99 | [110] |

*Note*: $R_f(5)$ and $R_r(5)$ indicate optimum values of shape fixity and shape recovery, respectively, after the fifth cycle

based on multiblock copolymers, where switching segments are covalently linked to the shape fixing segments. Blending and interpenetrating polymer network (IPN) forming strategies are often used to diversify the applications of polymer materials [108, 109]. Recently, polymer blends/IPNs based SMP and shape memory effect in ordered aggregates [110–112] (due to surfactant-charged gel interactions) have been investigated. It was reported that IPN-structured PEO ($M_w$ = 2000 g/mole)/poly(methyl methacrylate) (PMMA) systems show shape memory properties with two transition temperatures: one of them is due to the melting of PEO and the other is linked with the glass transition of the IPN [110].

## Biodegradable SMP

Since Lendlein and Langer [111] reported a PCL-based biodegradable polymer and demonstrated its potential in medical applications, biodegradable SMPs became under spot of considerable research interest. The biodegradable SMPs, reported so far are based on polyglycolide (PGA), poly(L-lactide) (PLLA) and PCL, which are well known biodegradable polymers mostly used in medical field [112, 113]. The advantage of biodegradable SMPs with PCL soft phase is that the recovery temperature can be adjusted to 37–40° C (close to human body temperature) by judicious selection of molecular weight of PCL, hard phase component and soft phase/hard phase compositions. The synthetic strategy for PCL-based SMP involves converting PCL to the corresponding diol as presented in Fig. 7. The diols can be reacted with an acrylic monomer to prepare PCL dimethacrylate which on photocuring gives an SMP network [114, 115] or the diols can be reacted with an isocyanate to make a polyurethane [116]. Various approaches are depicted in Fig. 10. Nagata et al. [117, 118] synthesized multiblock copolymer derived from PCL, 4,4-(adipoyl dioxy)dicinnamic acid and poly(ethylene glycol) (PEG), and studied their biodegradability and shape memory properties. PCL/PEG copolymers can exhibit outstanding combination of properties like hydrophilicity, permeability and degradability [119, 120]. It was reported that biodegradability increases with increase in PEG content due to the generation of less tight network as observed from the swelling study.

Lendlein et al. [114] investigated PCL-based dimethacrylates of different molecular weight. Mechanical and shape memory properties of PCL diacrylate samples are summarized in Table 6. Ping et al. [116] reported

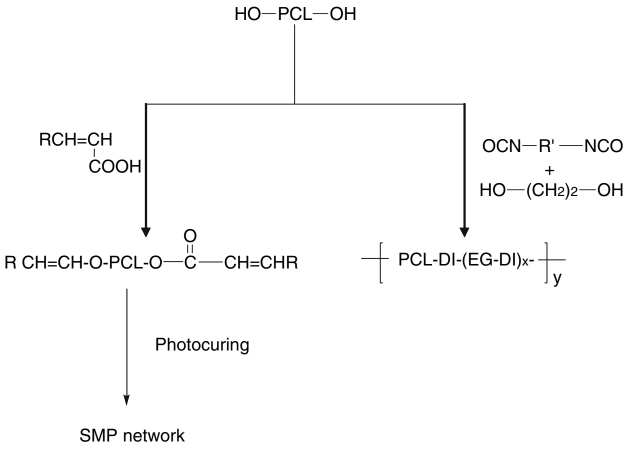

**Fig. 10** Description of synthetic strategies for biodegradable PCL-based SMP

**Table 6** Shape memory properties of biodegradable crosslinked PCL diacrylates [114]

| PCL Mol. wt g/mole | $E^a$ Mpa | $\varepsilon_m^a$ % | $R_r(2)$ % | $R_f(2)$ % |
|---|---|---|---|---|
| 1500 | 1.84 | 50 | 93.3 | 93.9 |
| 2000 | 2.20 | 50 | 96.3 | 93.9 |
| 3500 | 3.01 | 50 | 93.8 | 92.5 |
| 4500 | 2.30 | 50 | 98.6 | 86.3 |
| 6500 | 1.25 | 50 | 98.7 | 93.2 |
| 7000 | 1.91 | 150 | 98.1 | 95.0 |
| 10000 | 0.70 | 200 | 94.5 | 95.5 |

[a] At 70 °C; $R_f(2)$ and $R_r(2)$ indicate optimum values of shape fixity and shape recovery, respectively, after the second cycle

PCL-based polyurethane (PCLU) as shown in Fig. 10. Unlike the conventional way of stretching at or above $T_m$, they stretched the sample at 10–15° C lower than $T_m$ and allowed to recover at lower temperature. They argued that if specimen is deformed at $T_m$ or at a temperature higher than $T_m$, it should be quickly quenched to the room temperature to retain the deformed shape and to prevent the inner stress from releasing; otherwise the subsequent recovery will not be complete. When the deformation temperature is too low the shape recovery starts at lower temperature and takes place over a wide temperature range. The lowest recovery temperature (LRT) mostly depends on the molecular weight rather than the percentage hard segment as shown in Table 7.

The major limitations of PCL-based biodegradable SMPs are that the products after shape recovery are not strong enough for some practical applications and low biodegradation rate. Wang et al. [121] prepared PLA-based SMP in a similar approach (diol route) and evaluated the mechanical and shape memory properties. It was reported that PLA-based PU display better shape-memory behavior under a small deformation and more rapid response to the thermal stimuli. However, the $T_g$ of PLA is about 60 °C (much higher than body temperature) and hence, PLA-based SMP is not suitable for biomedical applications as they cannot recover near the body temperature. In order to address the above mentioned issues, random copolymers of PLA and PCL have been investigated [122]. The copolymer offers recovery temperature adjustment through PCL component and degradation rate adjustment through PLA component. Min et al. [123] reported shape memory polymers with PLA hard phase and poly(glycolide-co-caprolactone) (PGC) soft phase. Recently, a completely amorphous copolyester urethane network with shape memory property and biodegradability was reported [124]. Amorphous polymers offers the adequate transparency required for applications like ocular tissue [125, 126]. Kim et al. [127] reported shape memory effect of poly[3-hydroxybutyrate)-co-(3-hydroxy valerate)], which is a biodegradable polymer produced by the microorganisms. Thus biodegradable SMPs with good mechanical properties can be developed where the recovery temperature can be adjusted upon request for biomedical or other applications.

**Table 7** Thermal Properties of biodegradable PCL-based PU [116]

| PCL mol. wt g/mole | Hard segment % | $T_m$ °C | LRT °C |
|---|---|---|---|
| 2000 | 24.4 | 43 | 23.5 |
| 2500 | 20.5 | 45 | 27.1 |
| 3000 | 17.7 | 48.5 | 30.0 |
| 3500 | 31.2 | 50.4 | 33 |
| 5000 | 55.6 | 37.9 | 48 |
| 8000 | 60.5 | 45.4 | 51 |
| 10000 | 61.5 | 48.2 | 56 |

## SMP composites

The SMPs in general exhibit lower strength and stiffness, which limits their use for many advanced applications. The low stiffness of SMPs produces only a small recovery force in the temperature change process. Thus incorporation of reinforcing fillers have been investigated in order to improve the mechanical properties and to diversify the applications of SMPs [128, 129]. Liang et al. [130] investigated glass and Kevlar fiber reinforced SMP composites and observed increased stiffness and decreased recoverable strain as a result of incorporation of the reinforcements. Gall et al. [131] reported increase in elastic modulus by approximately a factor of 3, due to the incorporation of 40 wt% SiC. Ohki et al. [132] demonstrated the relationship between fiber weight fraction and recoverability for chopped strand glass fiber reinforced SMP composites, prepared by injection molding. The increase in failure stress of 140% and decrease in recovery rate of 62%, were reported as a result of addition of 50 wt% of glass fiber. Similar observation was reported for SMP composites by using carbon fiber reinforcement [133].

Conducting SMP composites have been reported by blending carbon black or a conducting polymer with the SMP [134, 135]. Recently, vapor grown carbon nanofibres reinforced SMP composites have been studied [136]. Incorporation of 3.3 wt% nanofibres resulted in 200% increase in recovery stress of the SMP composites. The nanocomposites retain high strain recoverability (more than 90%) after several cycles of training and going to be a subject of major focus in near future. Koerner et al. [137] investigated polyurethanes reinforced with carbon nanotubes (CNTs) or carbon black of similar size and reported that the nanocomposites display an increased shape fixity. The CNT-reinforced materials show almost 100% shape recovery compared to the material (reinforced with carbon black), which exhibit only a limited shape recovery of around 30%. The difference in behavior of the two materials, is attributed to the interactions between the anistropic CNT and the crystallizing PU switching segments [20]. The nanocomposites offer electrically induced actuation, which can be controlled remotely, via Joule heating when current is passed through the conductive percolative network of the nanotubes within the composite system.

SMP nanocomposites, in which shape memory effect can be triggered by magnetic field, have also been reported using a suitable magnetic nanofiller like $Fe_3O_4$ with a shell of oligo(e-caprolactone) [138] or Ni–Zn ferrite particles [139]. In these magnetic composites, the sample temperature is increased by the inductive heating of the nanoparticles in an alternating magnetic field ($f$ = 258 kHz, $H$ = 7–30 kAm$^{-1}$). The electromagnetic energy from the external high frequency field is transformed to heat due to the relaxation process. The effect was demonstrated for a PU-based SMP with an amorphous switching segment {aliphatic PU from methylene-bis (*p*-cyclohexyl isocyanate), 1,4-BD and polytetrahydrofuran}, as well as for a multiblock copolymer based SMP with PCL-based crystalline segment.

## Applications of SMPs

Potential applications for SMP exist in almost every area of daily life: from self repairing auto bodies to kitchen utensils, from switches to sensor, from intelligent packing to tools [66]. They can be used for heat shrinkable tube [140], auto repairing and self healing [141]. Other potential applications are drug delivery [142], biosensors, biomedical devices [143–146], microsystem components [147–151], and smart textile [152]. Since polymer can be made biodegradable they can be used as short term implants where removal by surgery can be avoided. Some important applications are discussed below in detailed.

Shape memory polymers have tremendous applications in biology and medicine [153, 154] especially for biomedical devices, which might permit new medical procedure. For example current approaches for implanting medical devices often require complex surgery followed by device implantation. However, with the development of minimally invasive surgery, it is possible to place small devices small device inside the body using a laparoscope. These types of surgical advances may create new opportunities to enable a bulky device to be implanted into the human body in a convenient way. Due to the ability of SMP to memorize a permanent shape that can be substantially different from an initial temporary phase, a bulky device could potentially be introduced into the body in a temporary shape like a string that could go through a small laparoscopic hole and then expanded on demand into a permanent shape at body temperature as shown schematically in Fig. 11.

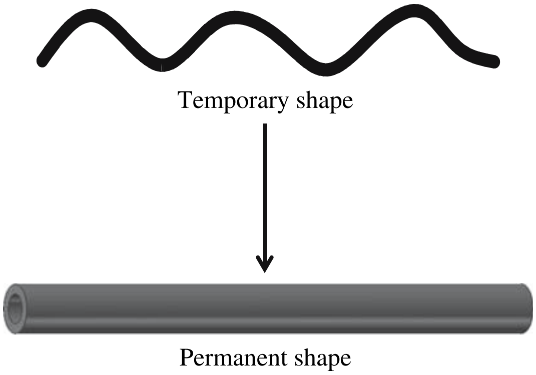

**Fig. 11** Representation of recovery of a string like material to a tubular device

Lendlein and Langer [154] reported a thermoplastic-elastomer-based SMP, which can be used as a smart suture. A challenge in endoscopic surgery is the tying of a knot with instruments and sutures, to close an incision or open lumen. It is especially difficult to manipulate the suture so that the wound lips are pressed together under the right stress. When the knot is fixed with a force that is too strong, necrosis of surrounding tissue can occur. If the force is too week, scar tissue, which has poorer mechanical properties forms and may lead to the formation of hernias. A possible solution is to design a smart surgical suture, whose temporary shape would be obtained by elongating the fiber with a controlled stress. The suture could be applied loosely in its temporary shape, when the temperature was raised above $T_s$ , the suture would shrink and tighten the knot, applying optimum force.

The SMPs have been proposed for stent application [155, 156] because of their high strain recovery without the adverse strain hardening effects encountered in metal stent expansion, facilitating delivery of larger devices through smaller delivery vehicles. Additional advantages of polymer-based stents include improved compliance matching, biodegradation capability, use of steriolithography for patient specific devices, and molecular surface engineering [157, 158]. Another area, in that polymer may prove useful, is the realm of pediatric stenting, in which metal stents can not be sufficiently expanded throughout the growth of patients [159, 160]. Recent work on design and performance evaluation of SMPs for cardiovascular stenting application shows a considerable promise [161]. The stent can be preprogrammed to activate at body temperature, resulting in natural deployment without a need for auxiliary devices (Fig. 12) [161].

The SMP has been proposed as a candidate for aneurysm coils [162]. An intracranial aneurysm can be a serious condition that could go undetected until the aneurysm ruptures, causing hemorrhaging within the subarachnoid space surrounding the brain. The typical treatment for large aneurysms is by remobilization using platinum coils. However, in about 15% of the cases treated by platinum coils, the aneurysm eventually re-opens as a result of the bio-inertness of platinum. One solution to this, is to develop suitable materials with increased bio-activity like SMPs to use as coil implants. Another example of a biomedical application is a microactuator made from thermosetting PU, which was used to remove blood vessel clots [22]. A microactuator, with a permanent shape of a cone-shape coil, can be elongated to a straight wire and fixed before surgery and delivered to a occlusion through a catheter. On triggering the shape recovery using an optical heating method, the original coil shape is recovered and the blood flow is restored [22, 163]. SMPs can be used to develop the devices (for orthodontic applications), which simplify the ligation and other time-intensive orthodontic procedures [164, 165]. SMPs have also been viewed for application [166, 167] as biodegradable intragastic implants that inflate after an approximate predetermined time and provide the patient with a feeling of satiety after only a small amount of food has been eaten. Thus a major health problem, obesity, caused by the overeating (especially in advanced country) can be addressed.

Shape memory polymers have potential to provide nanometer scale actuation. Nanometer scale imprints in SMP could be created with embossing and subsequently allowed to recover to provide actuation [168, 169]. Several applications of recoverable nanometer scale indents in shape memory polymers are possible namely covered nanoimprints on medical device could be used for small volume drug delivery. Alternatively, small scale imprints can be formed in the arrays to create an active nanostructured surface with an adjustable adhesion characteristic. Finally, active nanoprints could be used to position nanoparticles or nanowire. Nelson et al. [170] have created nanoscale imprints in an epoxy based SMP using an atomic force microscopy (AFM) tip and studied the indentation recovery as a function of time and temperature. The results are summarized in Table 8. It was found that at higher temperature (70° C) the indents are barely visible.

**Table 8** Effect of anneal temperature on peak-to-peak height [Data calculated from Graph, 170]

| Loading force, μN | Temperature, °C | Peak to peak height[a], nm |
|---|---|---|
| 70 | 25 | 27 |
| 70 | 60 | 12 |
| 70 | 65 | 11 |
| 70 | 70 | 04 |

[a] Peak-to-peak height is defined as the height difference between the deepest and highest feature in the indent. The deeper indentation made with higher-loading force recover faster than the shallower indents

Recently, a concept of cold-hibernated elastic memory utilizing SMPs in open cellular structures was proposed for space-bound structural application [171]. The concept of cold-hibernated elastic memory can be extended to a variety of new applications like microfoldable vehicles, shape determination and microtags [172]. Recent studies on shape memory polymer-based conductive composites using conducting polymer and carbon nanotube show

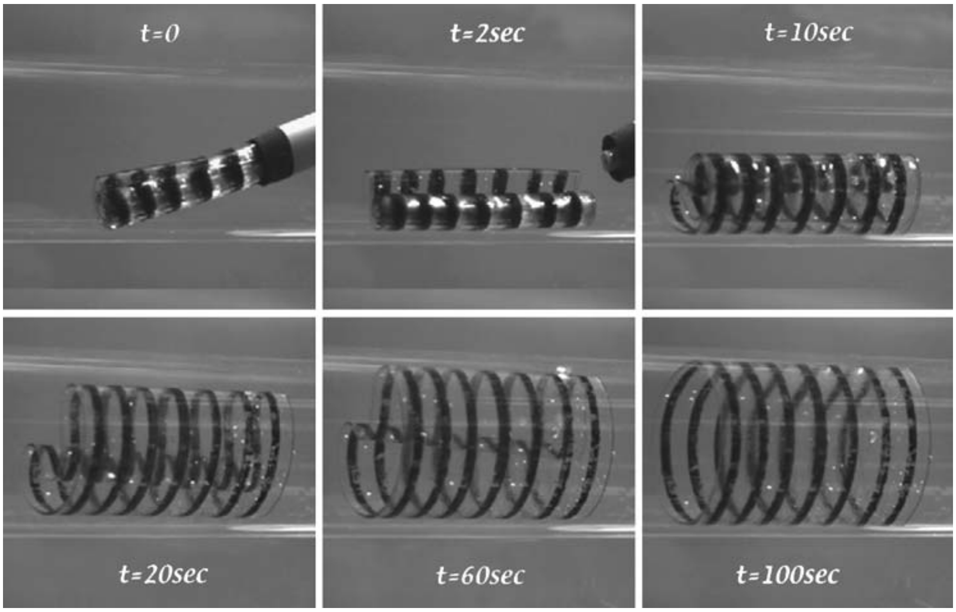

**Fig. 12** Recovery of a crosslinked SMP stent delivered via catheter into ID glass tube containing water at 37 °C [Reprinted with permission from Ref. 161 © 2007, Elsevier publishing company]

Fig. 13 Electroactive shape recovery behavior PU/polypyrrole system [Reprinted with permission from Ref 136 © 2005 Wiley-VCH Verlag GmbH & Co KgaA]

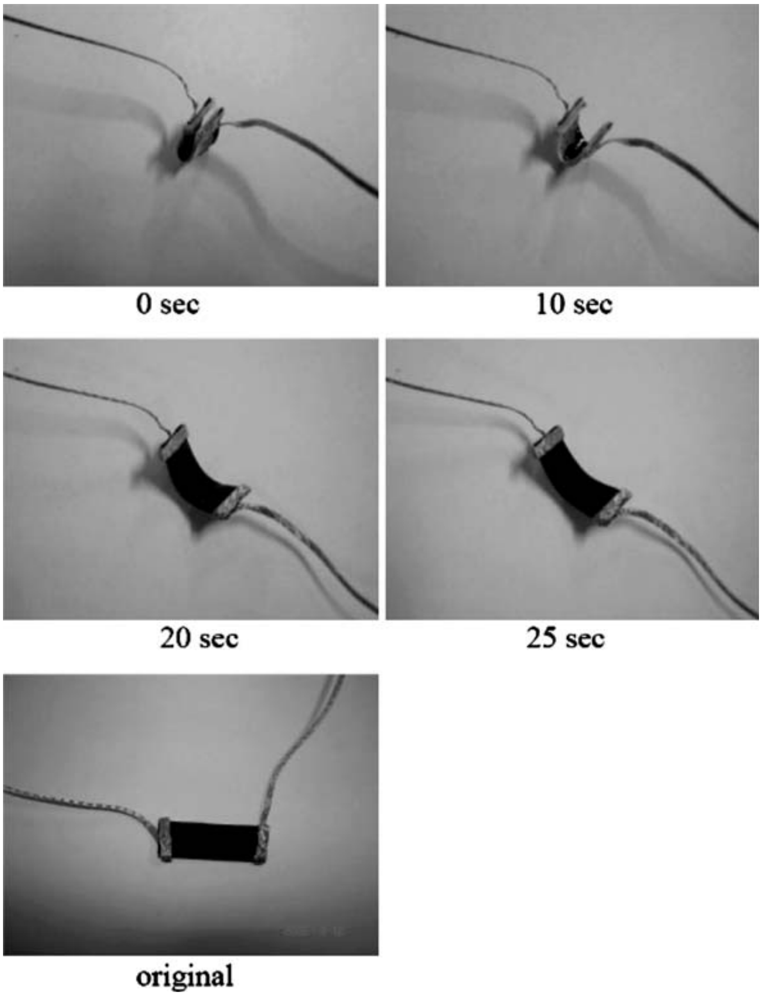

considerable promise for their application as electroactive and remote sensing actuators [135, 136]. An electroactive shape recovery of PU/polypyrrole composites is shown in Fig. 13.

## Summary and future outlook

In this article, the works reported in the literature on shape memory polymers have been reviewed highlighting the related issues and recent development. SMP can be designed by taking a polymer material (having both hard and soft or switching segment), in which the polymer chains are able to fix a given deformation by cooling below a certain transition temperature. Upon reheating to above $T_s$, the oriented chains in the network-restore the random coil conformation resulting in a macroscopic recovery to the original shape. Both thermoplastic (physical crosslink) and thermosetting (chemical crosslink) types of SMPs having crystalline or amorphous switching segments were discussed, majority of which are based on polyurethane systems. Physically crosslinked SMPs offer better processability and recyclability, on the other hand crosslinked SMPs offer better mechanical properties and better recoverability and reproducibility in terms of shape memory effect due to their inherent lower creep compared to thermoplastics. The SMPs, with crystalline switching segment, offer ease of fine tuning the recovery temperature, on the other hand SMPs, with amorphous switching segment, offer better transparency, which is very important for many applications. Biodegradable SMPs have been successfully synthesized and demonstrated for biomedical applications. Suitable biodegradable SMP can be designed with an optimum biodegradability and with adjusted recovery temperatures (for biomedical or any other applications) by judiciously selecting/developing the copolymer compositions based soft phase and hard phase.

In order to increase the versatility of SMPs, blending and interpenetrating network-based polymers have been investigated, which show considerable promise and going to be explored extensively in the future leading to the development of the newer and newer SMPs. SMPs are mostly thermoresponsive, however, attempts have been made to make the SMP systems, which can be induced by other means like light, magnetic field or electric current (which can be remotely controlled), by introducing respective switching segment in the molecular structure or by incorporating a suitable active filler. Such SMP structured systems, will find applications like remote sensing actuation and will open up many new fields of applications. SMPs are going to be the future materials for deployable structure for aircraft and spacecraft applications. The deployable thin film structure in a satellite, is to be folded using the hinges (made up of shape memory material) to save storage space and required to be opened to their full span, once deployed into the space by shape recovery of the hinges. The recovery process should be steady and well controlled as a fast recovery may vibrate the satellite in space. Design of suitable SMP for such strategic application can considerably decrease the weight of the space vehicle and reduce the cost.

**Acknowledgements** The first author (DR) is thankful to the Alexander von Humboldt (AvH) foundation for the grant of a post doctoral research fellowship. Authors are thankful to Elsevier and Wiley-VCH Verlag GmbH, for giving permission to reprint one figure each.

## References

1. Chang LC, Read TA (1951) Trans AIME 189:47
2. Buhler WJ, Gilfrich JW, Wiley RC (1963) J Appl Phys 34:1475
3. Wei ZG, Sandstrom R, Miyazaki S (1998) J Mater Sci 33:3743
4. Hornbogen E (2004) J Mater Sci 39:385
5. Feninat FE, Laroche G, Fiset M, Mantovani D (2002) Adv Eng Mater 4:91
6. Wataha JC, Hanks CT, Craig RG (1991) J Biomed Mater Res 25:1133
7. Humbeeck JV (2001) Adv Eng Mater 3:837
8. Shih CC, Lin SJ, Chen YL, Su YY, Lai ST, Wu GJ, Kwok CF, Chung KW (2000) J Biomed Mater Res 52:395
9. Uo M, Watari F, Yokoyama A, Matsumo H (2001) Biomaterials 22:677
10. Hornbogen E (2006) Adv Eng Mater 8:101
11. Swiain MV (1986) Nature 322:234
12. Schurch KE, Ashbee KHG (1977) Nature 266:706
13. Heuer AH, Ruhle M, Marshal DB (1990) J Am Ceram Soc 73:1084
14. Yu Y, Ikeda T (2005) Macromol Chem Phys 206:1705
15. Gould P (2007) Materials Today 10:10
16. Liu C, Qin H, Mather PT (2007) J Mater Chem 17:1543
17. Kim BS, Lee SH, Furukawa F (2005) In: Fakirov S (ed) Handbook of condensation thermoplastic elastomers. Wiley-VCH, Weinheim, pp 521–566
18. Behl M, Lendlein A (2007) Materials Today 10:20
19. CEER (1984) 16:34
20. Vaia R (2005) Nature Mater 4:429
21. Razzaq MY, Anhalt M, Frormann L, Weidenfeller B (2007) Mater Sci Eng A 444:227
22. Maitland DJ, Metzger MF, Schumann D, Lee A, Wilson TS (2002) Laser Surg Med 30:1
23. Finkelmann H, Nishikawa E, Pereira GG, Werner M (2001) Phys Rev Lett 87:15501
24. Lopez MC, Finkelmann H, Muhoray PP, Shelley M (2004) Nature Mater 3:307
25. Lendlein A, Jiang H, Junger O, Langer R (2005) Nature 434:879
26. Akabori S et al (1987) Bull Chem Soc Japan 60:3453
27. Tanka H, Hunda K (1977) J Polym Sci Polym Chem 15:2685
28. Tobushi H, Hayashi S, Kojima S (1992) Jap Soc Mech Engrs Int J 35:296
29. Lin JR, Chen LW (1999) J Appl Polym Sci 73:1305
30. Conti S, Lenz M, Rumpt M (in press) J Mech Phys Solid
31. Liu Y, Gall K, Dunn ML, Greenberg AR (2006) J Diani Int J Plasticity 22:279
32. Beloshenko VA, Varyukhin VN, Voznyak YV (2005) Composites A 36:65
33. Sharma BK, Gajaev IY, Mattiasson B (2000) Angew Chem Int Ed 39:2364
34. Poilane C, Delobele P, Lexcellent C, Hayashi S, Tobushi H (2000) Thin Solid Films 379:156
35. Kim BK, Lee SY, Xu M (1996) Polymer 37:5781
36. Yang F, Zang S, Li JCM (1997) Elect Mater 26:59
37. Nakyama K (1991) Int Polym Sci Technol 18:3
38. Jeon HG, Mather PT, Haddad TS (2000) Polym Int 49:453
39. Mather PT, Jeon HG, Uribe AR, Haddad TS, Lichtenhan JD (1999) Macromolecules 32:1194
40. Jeong HM, Song JH, Chi KW, Kim KT (2002) Polym Int 51:275
41. Sakurai K, Tanaka H, Ogawa N, Takahashi TJ (1997) J Macromol Sci B:Phys 36:703
42. Liang C, Rogers CA, Malafeew E (1997) J Intell Mater Struct 8:380
43. Lee C, Hwang J, Chae B (1994) US Pat 5,442,037
44. Tobushi H, Okumura K, Endo M, Hayashi S (2001) J Intelligent Mater Syst Struct 12:283
45. Tobushi H, Hoshimoto T, Ito N, Hayashi S, Yamada E (1998) J Intelligent Mater Syst Struct 9:127
46. Tobushi H, Hayashi S, Hoshio K, Makino Y, Miwa N (2006) J Intelligent Mater Sys Struct 17:1075
47. Baer G, Wilson TS, Mathews DL, Maitland DJ (2007) J Appl Polym Sci 103:3882
48. Hu JL, Ji FL, Wong YW (2005) Polym Int 54:600
49. Mondal S, Hu JL (2007) J Elast Plast 39:81
50. Takahashi T, Hayashi N, Hayashi S (1996) J Appl Polym Sci 60:1061
51. Kim H, Lee TJ, Huh JH, Lee DJ (1999) J Appl Polym Sci 73:345
52. Park HS, Kim JW, Lee SH, Kim BK (2004) J Macromol Sci B:Phys 43:447
53. Lee BS, Chun BC, Chung YC, Sul K, Cho JW (2001) Macromolecules 34:6431
54. Lin JR, Chen LW (1998) J Appl Polym Sci 69:1563
55. Lin JR, Chen LW (1998) J Appl Polym Sci 69:1575
56. Jeong HM, Lee SY, Kim BK (2000) J Mater Sci 35:1579
57. Chun BC, Cho TK, Chung YC (2007) J Appl Polym Sci 103:1435
58. Wang HH, Yuen U (2006) J Appl Polym Sci 102:607
59. Yang JH, Chun BC, Chung YC, Cho JH (2003) Polymer 44:3251
60. Cho JW, Jung YC, Chun BC, Chung YC (2004) J Appl Polym Sci 92:2812
61. Yang B, Huang WM, Li C, Li L (2006) Polymer 47:1348
62. Cho JW, Jung YC, Chung YC, Chun BC (2004) J Appl Polym Sci 93:2410
63. Kakursoin J, Agrawal AK (2007) J Appl Polym Sci 103:2172

64. Cha D, Kim HY, Lee KH, Jung YC, Cho JW, Chun BC (2005) J Appl Polym Sci 96:460
65. Jeong HM, Ahn BK, Kim BK (2001) Eur Polym J 37:2245
66. Jeong HM, Song JH, Lee SY, Kim BK (2001) J Mater Sci 36:5457
67. Kusy RP, Whitley JQ (1994) Thermochim Acta 243:253
68. Xu M, Li F (1999) Chin J Polym Sci 17:203
69. Li FK, Zhang XY, Wang MT, Ma DJ, Xu M, Luo XL, Ma DZ, Kim BK, (1997) J Appl Polym Sci 64:1511
70. Lendlein A, Kelch S, Kratz K (2006) Kunstoffe, 2:54
71. Jeong HM, Ahn BK, Kim BK (2000) J Polym Sci Polym B Phys 38:3009
72. Jeong HM, Lee JB, Lee SY, Kim BK (2000) J Mater Sci 35:279
73. Mandal S, Hu JL (2007) Carbohyd Polym 67:282
74. Jeong HM, Ahn BK, Kim BK (2000) Polym Int 49:714
75. Jeong HM, Kim BK, Choi YJ (2000) Polymer 41:1849
76. Han S, Gu BH, Nam KH, Im SJ, Kim SC, Im SS (2007) Polymer 48:1830
77. Zhu Y, Hu JL, Yeung KW, Liu YQ, Lien HM (2006) J Appl Polym Sci 100:4603
78. Zhu Y, Hu J, Yeung K, Choi K, Liu Y, Leim H (2007) J Appl Polym Sci 103:545
79. Chen S, Qi Cao, Jing B, Cai Y, Liu P, Hu J (2006) J Appl Polym Sci 102:5224
80. Fang ZQ (1996) China Elast 6:22
81. Chen S, Su J, Liu Chin P (2005) Chem Lett 16:1241
82. Rabani G, Luftmann H, Kraft A (2006) Polymer 47:4251
83. Ni X, Sun X (2006) J Appl Polym Sci 100:879
84. Sun X, Ni X (2004) J Appl Polym Sci 94:2286
85. Luo XL, Zang XY, Wang MT, Ma DZ (1997) J Appl Polym Sci 64:2433
86. Wang MT, Luo XL, Zang XY, Ma DZ, Zang LD (1997) Polym Adv Technol 8: 136
87. Wang M, Zhang L (1999) J Polym Sci Polym B Phys 37:101
88. Naga N, Tsuchiya G, Toyata A (2006) Polymer 47:520
89. Li F, Zhu W, Zhang X, Zhao C, Xu M (1999) J Appl Polym Sci 71:1063
90. Hu Z, Zhang X, Li Y (1995) Science 269:525
91. Skakalova V, Lukes V, Breza M (1997) Macromol Chem Phys 198:3161
92. Zhu G, Liang G, Xu Q, Yu Q (2003) J Appl Polym Sci 90:1589
93. Zhu G, Xu Q, Liang G, Zhou H (2005) J Appl Polym Sci 95:634
94. Li F, Larock RC (2002) J Appl Polym Sci 84:1533
95. Li F, Hasjim J, Larock RC (2003) J Appl Polym Sci 90:1830
96. Chang YW, Mishra JK, Cheong JH, Kim DK (in press). Polym Int
97. Rousseau IA, Mather PT (2003) J Am Chem Soc 125:15300
98. Zouohong Y, Jinlian H, Yeqiu L, Lapyan Y (2006) Mater Chem Phys 98:368
99. Hu J, Yang Z, Yeung L, Ji F, Liu Y (2005) Polym Int 54:584
100. Lee SH, Kim JW, Kim BK (2004) Smart Mater Struc 13:1345
101. Buckley CP, Prisacariu C, Caraculacu A (2007) Polymer 48:1388
102. Xu J, Shi W, Pang W (2006) Polymer 47:457
103. Chen W, Zhu C, Gu X (2002) J Appl Polym Sci 84:1504
104. Kim BK, Park SH (1999) J Polym Sci A:Chem 37:2703
105. Park C, Lee JY, Chun BC, Chung YC, Cho JW, Cho BG (2004) J Appl Polym Sci 94:308
106. Chun BC, Cha SH, Chung YC, Cho JW (2002) J Appl Polym Sci 83:27
107. Chun BC, Cha SH, Park C, Chung YC, Cho JW (2003) J Appl Polym Sci 90:3141
108. Liu G, Ding X, Cao Y, Zheng Z, Peng Y (2004) Macromolecules 37:2228
109. Liu G, Guan C, Xia H, Guo F, Ding X, Peng Y (2006) Macromol Rapid Commun 27:1100
110. Liu G, Ding X, Cao Y, Zheng Z, Peng Y (2005) Macromol Rapid Commun 26:649
111. Lendlein A, Kelch S, (2002) Angew Chem Int Ed 41:2034
112. Jain RA (2000) Biomaterials 21:2475
113. Abayasinghe NK, Perera KPU, Thomas C (2004) J Biomater Sci Polym Ed 15:595
114. Lendlein A, Schmidt AM, Schroeter M, Langer R (2005) J Polym Sci A Chem 43:1369
115. Bertmer M, Alina B, Hofgess IB, Kelch S, Lendlein A (2005) Macromol Symp 230:110
116. Ping P, Wang W, Chen X, Jing X (2005) Biomacromolecules 6:587
117. Nagata M, Kitazima I (2006) Colloid Polym Sci 284:380
118. Nagata M, Sato Y, (2005) J Polym Sci A Chem 43:2426
119. Petrova PS, Manolova N, Rashkov I, Li S, Vert M (1998) Polym Int 45:419
120. Cohn D, Stern T, Gonzalez F, Epstein J (2002) J Biomed Mater Res 59:273
121. Wang W, Ping P, Chen X, Jing X (2006) Eur Polym J 42:1240
122. Wang W, Ping P, Chen X, Jing X (2007) J Appl Polym Sci 104:4182
123. Min C, Cui W, Bei J, Wang S (2005) Polym Adv Technol 16:608
124. Alteheld A, Feng Y, Kelch S, Lendlein A (2005) Angew Chem Int Ed 44:1188
125. Liu L, Sheardown H (2005) Biomaterials 26:233
126. Williams DF, (2003) Sadhana 28:563
127. Kim YB, Chung CW, Kim HW, Rhee Y (2005) Macromol Rapid Commun 26:1070
128. Gall K, Dunn ML, Liu Y, Finch D, Lake M, Munshi NA (2002) Acta Mater 50: 5115
129. Park YC, Lee JK, Lee GC (2007) Compos Struct 77:241
130. Liang C, Rogers CA, Malafeew E (2000) J Intelligent Mater Syst Struct 11:877
131. Liu Y, Gall K, Dunn ML, McCluskey P (2004) Mech Mater 36:929
132. Ohki T, Ni QQ, Ohsako N, Iwamoto M (2004) Composites A 35:1065
133. Zhang CS, Ni QQ (2007) Compos Struct 78:153
134. Ni QQ, Zhang CS, Fu Y, Dai G, Kimura T (2007) Compos Struct 81:176
135. Cho JW, Kim JW, Jung YC, Goo NS (2005) Macromol Rapid Commun 26:402
136. Sahoo NG, Jung YC, Goo NS, Cho JW (2005) Macromol Mater Eng 290:1049
137. Koerner H, Price G, Pearce NA, Alexander M, Vaia R (2004) Nature Mater 3:115
138. Mohr R, Kartz K, Weigel T, Luka-Gabor M, Moneke M, Lendlein A (2006) PNAS 103:3540
139. Schmidt AM (2006) Macromol Rapid Commun 27:1168
140. Kleinhans G, Starkl W, Nuffer K, (1986) Kunststoffe 76:1069
141. Dietsch B, Tong T (2007) J Advanced Mater 39:3
142. Metcalfe A, Desfaits AC, Salazkin I, Yahia LH, Sokolowski WM, Raymond J (2003) Biomaterials 24:491
143. Metzger MF, Wilson TS, Schumann D, Mathew DL, Maitland DJ (2002) Biomed Microdevices 4:89
144. Small W, Wilson T, Benett W, Loge J, Maitland DJ (2005) Opt Express 13:8204
145. Wache HM, Tartakowska DJ, Hentrich A, Wagner MH (2003) J Mater Sci Mater Med 14:109
146. Gall K, Yakacki CM, Liu Y, Shandas R, Willet N, Anseth KS (2005) J Biomed Mater Res A 73:339
147. Gall K, Mikulas M, Munsi N, Tupper M (2000) J Intelligent Mater Syst Struct 11:877
148. Langer RS, Lendlein A (2002) US Patent 6,388,043 B1

149. Sokolowski WM, Chmielewski AB, Hayashi S, Yamada T (1999) Proceeding of SPIE-the international society for optical engineering; electroactive Polym. Actuator Devices. pp 179–185
150. Monkman G (2000) J Mechatronics 10:489
151. Ken G, Paul K, Dravid T, Michael H (2004) J Microelectromechanical Syst 13:472
152. Enomoto M, Suehiro K (1997) Text Res J 67:601
153. Langer R, Tirrell DA (2004) Nature 428:487
154. Lendlein A, Langer R (2002) Science 296:1673
155. Tamai H, Igaki K, Kyo E, Kasuga K, Kawashima A, Matsui S (2000) Circulation 102:399
156. Vogt F, Stein A, Rettemeier G, Krott N, Hoffmann R, Dahl V (2004) Eur Heart J 25:1330
157. Palmaz JC (2004) J Endovas Therapy 11:200
158. Cooke MN, Fisher JP, Dean D, Rimnac C, Mikos AG (2003) J Biomed Mater Res B: Appl Biomater 64B:65
159. Ewert P, Riesenkampff E, Neuss M, Kretschmar O, Nagdyman N, Lange PE (2004) Catheteriz Cardiovasc Intervent 62:506
160. Epstein ML, (2004) Catheteriz Cardiovasc Intervent 62:511
161. Yakacki CM, Shandas R, Lanning C, Rech B, Eckstein A, Gall K (2007) Biomaterials 28:2255
162. Hampikian JM, Heaton BC, Tong FC, Zhang Z (2006) Mater Sci Eng C 26:1373
163. Small WIV, Metzer MF, Wilson TS, Maitland DJ (2005) Quantam Electron 11:892
164. Mather PT, Liu C, Brustone CJ (2006) Shape memory polymer orthodontic appliances and methods of making and using the same. WO 2006/071520
165. Behl M, Lendlein A (2007) Soft Matter 3:58
166. Maco D (2006) Biodegradable self inflating intragestic implants for curbing appetite. WO 2006/092789 A2
167. Lendlein A, Langer RS (2004) Self expanding device for the gastrointestinal or urogenital area. WO 2004/073690 A1
168. Chou SY, Krauss PR, Ronstrom PJ (1996) Science 72:85
169. King WP, Kenny TW, Goodson KE, Cross GLW, Despont M, Durig U, Rothuizen H, Binning G, Vettiger P (2001) Appl Phys Lett 78:1300
170. Nelson BA, King WP, Gall K (2005) Appl Phys Lett 86103108
171. Tey SJ, Huang WM, Sokolowski WM (2001) Smart Mater Struct 10:321
172. Huang WM, Lee CW, Teo HP (2006) J Intel Mater Sys Str 17:753